Modeling Variable-Impedance, Magnetically Insulated Transmission Lines

R. B. Spielman and A. B. Sefkow

Laboratory for Laser Energetics, University of Rochester

The design of very-low-inductance, magnetically insulated transmission lines (MITL's) is a critical part of building low-inductance vacuum transmission lines and load configurations. It becomes more difficult to build low-impedance (low-inductance), constant-impedance MITL's when the MITL's must operate at high voltage. This is due to the increase in the fraction of the electrical current carried in vacuum electron flow in the MITL's at high voltage. Vacuum electron flow can be lost at downstream locations with impedance mismatches and at vacuum convolutes. We describe the design of a variable-impedance, disk MITL that allows us to reduce the inductance of disk MITL's. In this design, the impedance of the MITL at a radius of r = 150 cm is at 1.5 Ω, while the impedance of the MITL at a radius of r = 30 cm is 2 Ω. The impedance transition between these two radial locations can be done many ways but this summary uses a simple linear change in gap from the outer 1.5-Ω MITL to the inner 2.0-Ω MITL. Two-dimensional, electromagnetic (EM) particle-in-cell (PIC) simulations of this variable-impedance MITL will show electron flow and losses.

Our variable-impedance MITL is a conical disk MITL that starts at a radius of r = 150 cm and proceeds inward to a radius of r = 30 cm (see Fig. 1). The initial geometric impedance is 1.5 Ω (at 150 cm) with a gap of dz = 3.76 cm. The final geometric impedance is 2 Ω (at 30 cm) with a gap of dz = 1 cm. The inductance of this variable-impedance, disk MITL is 6.52 nH, a reduction of 1.55 nH when compared with an 8.07-nH, 2-Ω disk MITL. We now clearly see the reason for a variable-impedance MITL—lower inductance leading to higher efficiencies. The 2-Ω MITL design was described by Spielman and Reisman,[1] where a Z-flow model was used to quantify the vacuum electron flow at peak MITL voltage. The circuit code *Screamer*[2] was used to model

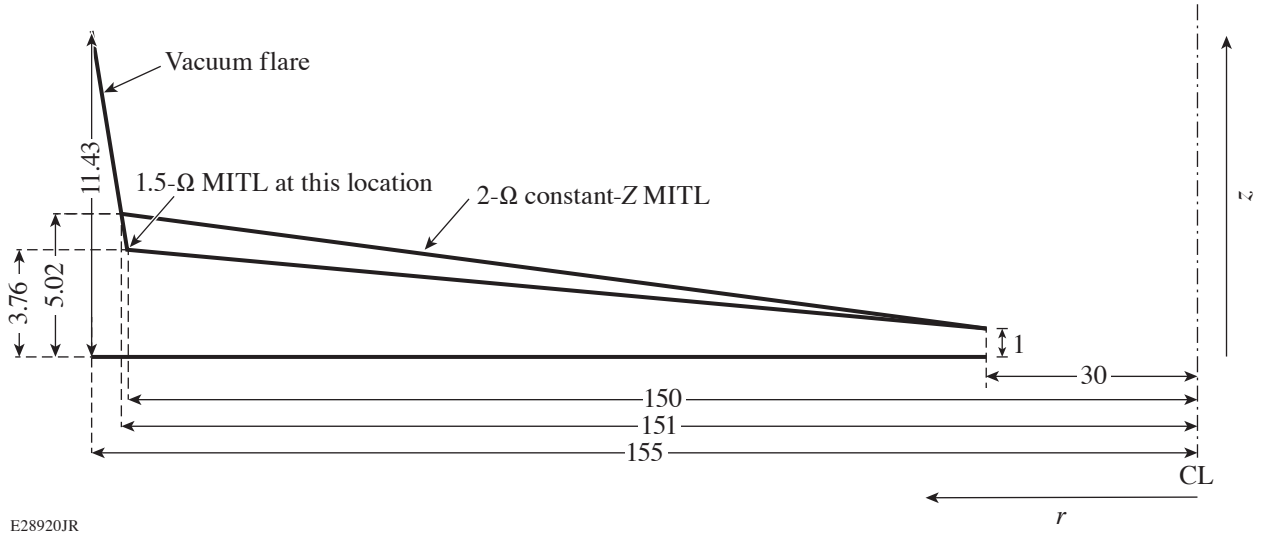

Figure 1
We show a schematic of a conical-disk MITL having a constant, 2-Ω impedance MITL profile and a similar conical-disk MITL having a variable, 1.5-Ω to 2-Ω impedance MITL profile. The figure shows a slice of the MITL at a single rotational angle around the marked center line. All units are in cm. CL: center line.

the qualitative MITL performance in Ref. 1. Herein, we model electron losses that will occur in a well-behaved, superinsulated variable-impedance disk MITL operating with equilibrium, vacuum electron flow. While we know that *any* variable-impedance MITL will have losses,[3] we assert that the real question is the magnitude of such losses.

The analytic approach to modeling electron losses in a variable-impedance MITL is based on the Z_{flow} model for MITL's described by Ottinger *et al.*[4] We assume as a worst case that any change in vacuum electron flow in excess of the retrapping current seen in the constant, the 2-Ω impedance case is lost at each segment transition. A 2-Ω MITL, as modeled here, has a slowly dropping vacuum electron flow moving inward due the nonmatched load. This forces retrapping of some of the vacuum electron flow. In reality, these loss currents are not at the discrete segment boundaries but are distributed over the entire MITL. The peak vacuum flow in the variable-impedance case is ~4% of the total anode current (in the outer MITL segment). The loss currents range from 3.4 kA on the outer segment to 6.2 kA on the inner segment. Importantly, the increase in total current due to the reduced inductance exceeds the increase in vacuum flow by 3×.

This particular impedance profile (linear in gap, not linear in Z) is not the optimum profile for pushing electron losses radially outward, where they have less impact due to the larger surface area. Various impedance profiles are possible and some of these have lower inductance than others. It is important to note that these predicted variable-impedance loss currents are significantly lower than the current losses seen during the setup of magnetic insulation.[1] It should be obvious that a variable-impedance MITL with a larger change in impedance (e.g., 1 Ω to 2 Ω) would suffer larger electron losses. Eventually, the losses in a variable-impedance MITL due to large impedance changes would approach the current losses seen during the setup of magnetic insulation and possibly result in MITL failure due to anode heating.

A 2-D EM PIC code can provide a more-quantitative picture of the electron losses in a variable-impedance MITL. For numerical accuracy, the number of macroparticles must be kept large (poor run time). The *LSP* code[5] is used to model the electron flow in the MITL's.

In *LSP*, the voltage waveforms generated in *Screamer* calculations are used as input to the simulation. The physical geometry of the MITL is as described earlier in Fig. 1. *LSP* invokes a unipolar, Child–Langmuir emission model that starts electron emission from the cathode at 200 kV/cm. An adaptive particle management routine is used to maintain about 100 particles per cell, resulting in a few million total macroparticles in the calculation. Radial resolution is ~1000 μm and axial resolution is ~100 μm.

We first ran a simulation with a constant-impedance 2-Ω MITL. In this case we do not expect losses in the constant-impedance section of the MITL. Figure 2 shows a snapshot of the electron density in the simulation at 100 ns, the time where the voltage is maximum and the current has reached half its peak. The Z-flow MITL theory predicts this MITL is perfectly insulated at peak voltage with no electron losses. The dz thickness of the vacuum sheath will decrease slightly as one moves from larger to smaller radius. The simulation is then rerun with identical electrical parameters except for the geometric boundary change of the variable-impedance disk MITL. The MITL impedance varies from 1.5 Ω at R = 150 cm and 2 Ω at R = 30 cm. For comparison, Fig. 3 shows the analogous snapshot of the variable-impedance MITL simulation at 100 ns.

One can now compare the two simulations. First, the small vortices that form in Fig. 2 appear to be influenced by the stairstep profile found on the MITL anode. Use of a surface-conformal meshing technique in these simulations would allow full clarification of this point. An examination of the electron flow in Fig. 3 shows similar vortices that are larger in amplitude and shorter in wavelength than those in Fig. 2. One can see that the thickness of the electron sheath at large radius is thicker in Fig. 3 than in Fig. 2. This is expected since the lower-impedance MITL modeled in Fig. 3 should have the larger sheath. Examination of multiple time steps of both simulations shows that these vortices have rotational flow (counterclockwise). It is interesting to note that the thickness of the electron sheath between the vortices is as expected in Fig. 3. The higher impedance at smaller radius results in the same electron sheath thickness as the constant 2-Ω case.

Importantly, there are no increased electron losses to the anode at the time of peak voltage in the variable-impedance case. This is true even though we have used a poor impedance profile with radius, where the use of a geometric straight line has greater dZ/dr at smaller radius and so should develop more losses at smaller radii. More-favorable dZ/dr profiles would reduce or eliminate the dZ/dr at small radius and push the changes in Z to larger radii, where losses are significantly less consequential.

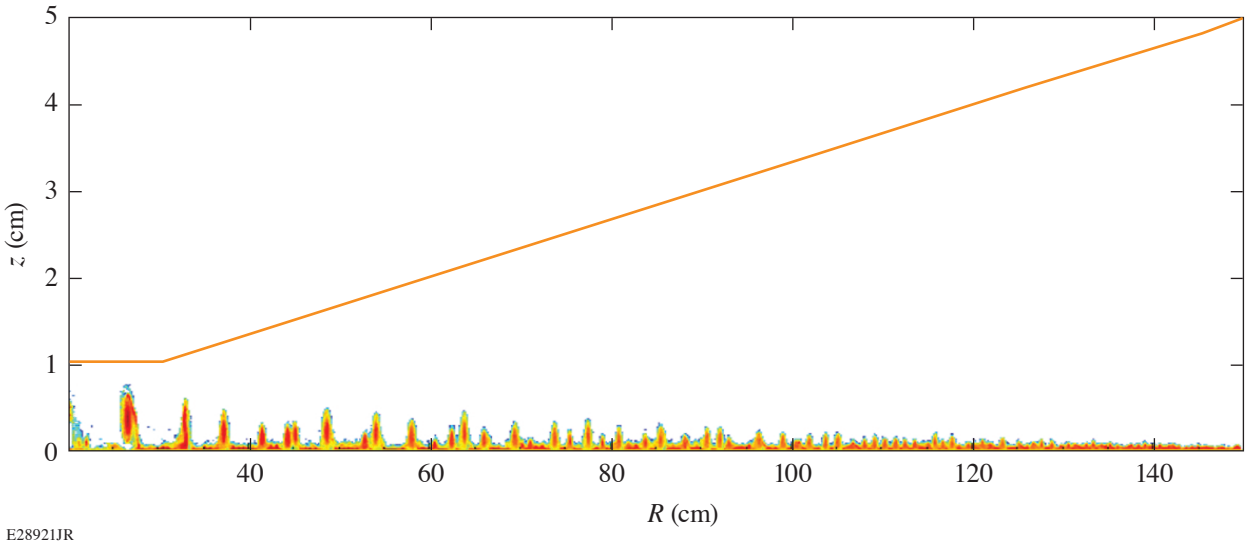

Figure 2
A snapshot of constant-impedance (2-Ω) MITL performance at $t = 100$ ns, where the simulation is at peak voltage and 0.5× maximum current.

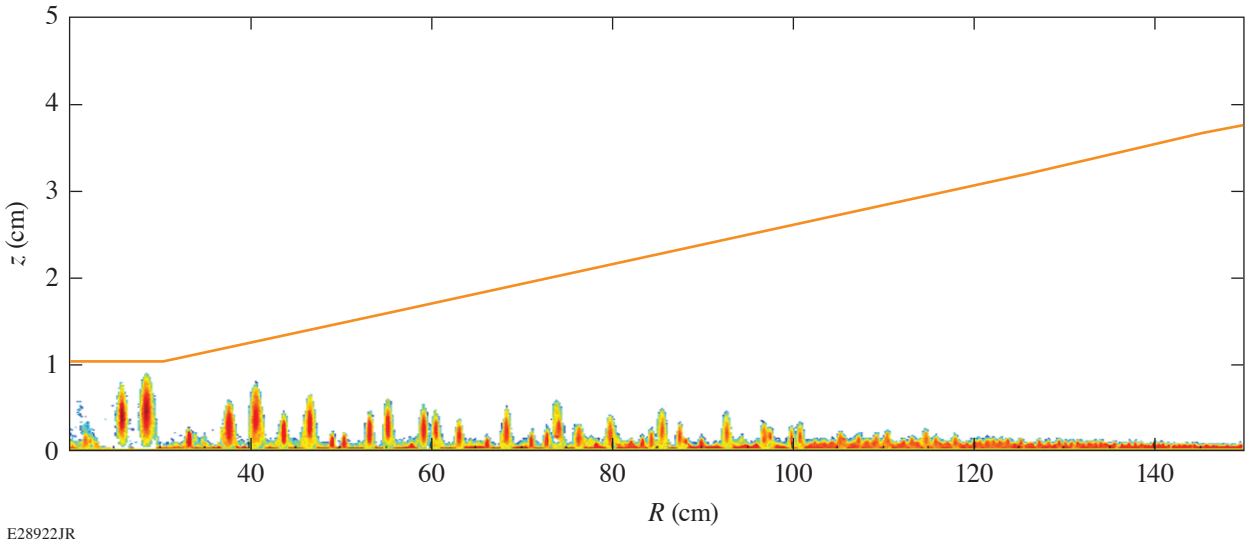

Figure 3
A snapshot of variable-impedance (1.5-Ω to 2-Ω) MITL performance at $t = 100$ ns, where the simulation is at peak voltage and 0.5× maximum current.

This material is based upon work supported by the Department of Energy National Nuclear Security Administration under Award Number DE-NA0003856, the University of Rochester, and the New York State Energy Research and Development Authority.

1. R. B. Spielman and D. B. Reisman, Matter Radiat. Extremes **4**, 027402 (2019); **4**, 049901(E) (2019).

2. R. B. Spielman and Y. Gryazin, in *2015 IEEE Pulsed Power Conference (PPC)* (IEEE, Piscataway, NJ, 2015).

3. T. D. Pointon and M. E. Savage, in *2005 IEEE Pulsed Power Conference* (IEEE, Piscataway, NJ, 2005), pp. 151–154.

4. P. F. Ottinger *et al.*, in *17th IEEE International Pulsed Power Conference*, edited by R. D. Curry (IEEE, Piscataway, NJ, 2009), pp. 1176–1179.

5. D. V. Rose *et al.*, Phys. Rev. Spec. Top., Accel. Beams **18**, 030402 (2015).